RSC Advances

PAPER

View Article Online
View Journal | View Issue

Cite this: *RSC Adv.*, 2023, **13**, 26001

Characterization and antimicrobial activity of a chitosan-selenium nanocomposite biosynthesized using *Posidonia oceanica*†

Wessam A. Abd-Elraoof,[a] Ahmed A. Tayel,[a] Shaymaa W. El-Far,[b] Omar Mohamed Walid Abukhatwah,[c] Amany M. Diab,[d] Osama M. Abonama,[e] Mona A. Assas[a] and Asmaa Abdella*[e]

Nanobiotechnological approaches can provide effective solutions for overcoming food products' contamination and spoilage. The development of rapid and eco-friendly approaches for synthesizing nanocomposites from chitosan nanoparticles (Cht), Neptune grass "*Posidonia oceanica*" extract (NG), and NG-mediated selenium nanoparticles (SeNPs) was targeted, with their investigation as potential antimicrobial, antioxidant, and biopreservatives of fresh chicken fillets. SeNPs were biosynthesized with NG, and their conjugates with Cht were composited. Characterization approaches, including infrared analysis, physiognomic analysis, and electron microscopy of synthesized nanomaterials and composites, were applied. The nanomaterials' antibacterial properties were assessed against *Staphylococcus aureus*, *Salmonella typhimurium*, and *Escherichia coli* qualitatively, quantitatively, and with ultrastructure imaging. The antimicrobial and antioxidant potentialities of nanomaterials were employed for preserving chicken fillets, and the sensorial and microbiological parameters were assessed for coated fillets. SeNPs were effectively biosynthesized by NG, with mean diameters of 12.41 nm; the NG/SeNPs had homogenous spherical shapes with good distribution. The prepared Cht/NG/SeNPs nanoconjugates had a mean diameter of 164.61 nm, semi-spherical or smooth structures, and charges of +21.5 mV. The infrared analyses revealed the involvement of biochemical groups in nanomaterial biosynthesis and interactions. The antibacterial actions of nanomaterials were proven against the entire challenged strains; Cht/NG/SeNPs was the most active agent, and *Salmonella typhimurium* was the most susceptible bacteria. Scanning micrographs of Cht/NG/SeNPs-treated *Staphylococcus aureus* and *Salmonella typhimurium* indicate the severe time-dependent destruction of bacterial cells within 8 h of exposure. The antioxidant potentiality of Cht/NG/SeNPs was the highest (91.36%), followed by NG/SeNPs (79.45%). The chicken fillets' coating with Cht, NG, NG/SeNPs, and Cht/NG/SeNPs resulted in a remarkable reduction in microbial group count and raised the sensorial attributes of coated fillets after 14 days of cold storage, with increased potentialities in the order: Cht/NG/SeNPs > NG/SeNPs > NG > Cht > control. The inventive, facile biosynthesis of Cht, NG, and SeNPs could provide effective antimicrobial and antioxidant nanocomposites for prospective applications in food biopreservation.

Received 29th June 2023
Accepted 25th August 2023

DOI: 10.1039/d3ra04288j

rsc.li/rsc-advances

1. Introduction

Selenium is a nutritional element with several biological functions and is an essential cofactor of antioxidant enzymes protecting the human body against free radicals.[1] Numerous pharmacological effects of selenium include immunomodulatory abilities, cellular metabolism, and involvement in the control of thyroid hormone metabolism.[2] It also has antibacterial, antifungal, antiviral, anticancer, and antioxidant properties. Selenium effectiveness was validated for protection from kidney, liver, and heart oxidative damage.[3] Selenium nanoparticles (SeNPs) have exceptional physicochemical properties such as low toxicity, biocompatibility, and chemical stability compared to inorganic selenium.[4] Additionally, selenium nanoparticles (SeNPs) exhibit size-dependent consequences;

[a]*Department of Fish Processing and Biotechnology, Faculty of Aquatic and Fisheries Sciences, Kafrelsheikh University, Kafr El Sheikh city 33516, Egypt*

[b]*Department of Pharmaceutics and Industrial Pharmacy, Division of Pharmaceutical Microbiology, College of Pharmacy, Taif University, Taif 21944, Saudi Arabia*

[c]*Cardiology & Internal Medicine Resident, Alexandria University Hospital, Egypt*

[d]*Department of Aquaculture, Faculty of Aquatic and Fisheries Sciences, Kafrelsheikh University, Kafr El Sheikh city 33516, Egypt*

[e]*Department of Industrial Biotechnology, Genetic Engineering and Biotechnology Research Institute, University of Sadat City, El-Sadat City 22857, Egypt. E-mail: asmaa.abdelaal@gebri.usc.edu.eg*

† Electronic supplementary information (ESI) available. See DOI: https://doi.org/10.1039/d3ra04288j

smaller particles are physiologically more active and aggregate better in tissues.[5] The absorptions and bioavailabilities of active ingredients may be improved after being formulated into the nanoscale.[6] The antimicrobial activity of SeNPs was found to be greater than that of inorganic selenium.[7] SeNPs have advantages over traditional antimicrobial agents in overcoming bacterial drug resistance mechanisms such as slow drug uptake, accelerated efflux, and biofilm formation.[8] SeNPs were highly effective for augmenting the bioactivities of glutathione peroxidase and thioredoxin reductase.[9]

SeNPs in aqueous solution were susceptible to aggregation into large clusters, resulted in a lower bioactivity and bioavailability.[1,3,5] The nanocomposites (NCs) of SeNPs and organic polymer were fabricated to increase its medicinal activity such as directed delivery to diverse organs, and sustained release.[10] One of the most promising polymers for creating such a biologically active NCs is chitosan due to its nontoxicity, biocompatibility, sustainable supply, simple extraction and other polyfunctional properties.[11] Chitosan nanoparticles (Cht) have a unique characteristic, which augments permeability of hydrophilic materials.[12] Cht were proved to enhance the bioactivities (*e.g.* antimicrobial, anticarcinogenic, anti-inflammatory, antiviral and antioxidant activities) of metal nanoparticle.[13]

There are three methods for the preparation of SeNPs, which are the physical, chemical, and biological methods.[14] Biological methods are preferred because they are ecofriendly, more cost-effective than other alternatives, and biocompatible for pharmaceutical manufacturing and other biomedical applications.[1,3] Biogenic or green synthesis of SeNPs can be done using organisms such as fungus, algae, bacteria, and plants, as well as their metabolites, which function as reducing and stabilizing agents.[5,9,14] *Posidonia oceanica*, known as Neptune grass (*Posidoniaceae*), is a Mediterranean Sea grass.[15] *P. oceanica* was used for the synthesis of metallic nanoparticles.[16] Phenolic acids (including 4-hydroxybenzoic, coumaric, gentisic, cinnamic, chicoric, and ferulic acids) and flavonoids (*e.g.*, quercetin, kaempferol, myricetin, and isorhamnetin) in *P. oceanica* extracts (NG) have been employed as reducing and stabilising agents in the biosynthesis of nanoparticles.[17] For its promising benefits, *P. oceanica* has attracted interest in healthcare applications, mostly associated with the antiradical and antioxidant actions of plant phenolic components.[18]

The development of edible coatings (EC) in packaging approaches succeeded in extending foodstuffs shelf-lives. EC is defined as "thin layers of materials that cover food surfaces and can be eaten and considered as a part of the overall food product." Natural edible coatings are environmentally friendly and can boost goods' quality. Numerous foodstuffs (*e.g.*, fresh fruits, meats, vegetables,… *etc.*) were effectively preserved with ECs, which comprised diverse biomolecules/polymeric agents, including lipids, polysaccharides and proteins.[11,13] No published papers are available concerning the biosynthesis of Cht/NG/SeNPs nanocomposite using *P. oceanica* yet. Accordingly, we aimed to: (i) synthesize Cht/NG/SeNPs; (ii) investigate the physiochemical and structural characteristics of Cht/NG/SeNPs nanocomposite; (iii) assess the antibacterial and antioxidant activities of biosynthesized NCs; (iv) evaluate the sensory, microbial, and chemical attributes of preserved poultry fillets coated with biosynthesized Cht/NG/SeNPs.

2. Materials and methods

2.1. *Posidonia oceanica* collection and identification

Posidonia oceanica (Neptune grass) leaves were collected from grasses blooming at the coast of the Mediterranean Sea near Marsa Matrouh, Egypt (Fig. 1). The grass was discovered and identified in the "Faculty of Aquatic and Fisheries Sciences, Kafrelsheikh University" to eliminate any salts or sand, the seagrass was cleansed and rinsed extensively with deionized water (DW). After that, the grasses were dried at 432 °C for 52 h, pulverized, and stored at room temperature (RT).

2.2. Preparation of *P. oceanica* extract

The leaf powder of *Posidonia oceanica* was extracted by maceration in 10 folds of 70% ethanol overnight at 37 ± 1 °C, under stirring (190*g*). After filtration, the Neptune grass extract (NG) was vacuum evaporated at 42 ± 1 °C until dryness. The dried NG powder was reconstituted in DW, vortexed, and filtered.

2.3. Phytosynthesis of SeNPs using *P. oceanica* extract

An equal volume of NG (0.1%, w/v) and 20 mM Na_2SeO_3 solutions were combined and stirred in the dark (720*g* for 35 min) at RT. Then, an aqueous solution of ascorbic acid (50 mM) was added dropwise to the previous solutions. To finish the reduction process, the reaction mixtures were stirred with a magnetic stirrer for 60 minutes. The change of the solution's colour from pale yellow to orange-red indicated the synthesis of SeNPs by NG. The formed nanoparticles (NPs) were collected *via* centrifugation (10 700*g* for 18 min), lyophilized, and kept at RT.[19] The plain SeNPs were attained *via* recurrent DIW-centrifugation cycles (5 times) to eliminate most of capping NG.

2.4. Extraction of chitosan

The shells' waste of *Erugosquilla massavensis* (mantis shrimp) were utilized as sources to extract chitosan. Wastes were attained from "Seafoods processing plants, Kafrelsheikh University, Egypt", they were cleansed, washed with DW and dried (55 ± 3 °C) for 20 h. After shells' grinding, chitosan extraction was executed, which involved demineralization (treatment with 16 folds of 1 M HCl, 12 h, RT); deproteinization (treatment with 16 folds of 1 M NaOH, 12 h, RT); and deacetylation (treatment with 18 folds of 55% NaOH solution, 95 min, 115 °C). Extensive DW washing and drying followed each step, and the final powder was preserved for analysis.[11,20]

2.5. Synthesis of Cht/NG/SeNPs nanocomposites

Chitosan powder was dissolved in 0.15% (v/v) aqueous acetic acid to get concentrations of 1% (w/v). The NG/SeNPs solution of 0.1% was also prepared in DW, then equal volumes were mixed from the above solutions and stirred (480*g*, 45 min). Sodium tripolyphosphate (TPP) with 0.5% concentration was dropped into 50 mL of the mixture solution within an hour with continuing

Fig. 1 Seagrass (*Posidonia oceanica*) bloom and close image of plant materials.

stirring.[21] Multiple centrifugations (3 times, 10 700*g*, 28 min) with DW washing were applied for harvesting the generated Cht from chitosan, NG, and SeNPs, which were then lyophilized. For the plain Cht preparation, TPP solution was dropped into the chitosan solution, and the subsequent steps were applied.

The entire nanometals/NCs were lyophilized and their powders we reconstituted in DW at 1.0% concentration (w/v), sonicated for 15 min and employed for further analysis and experiments, after appropriate dilutions with DW when required.

2.6. Characterization

2.6.1 Fourier transform infrared spectroscopy (FTIR) analysis. The powders of NG, SeNPs, Cht, and Cht/NG/SeNPs nanocomposite were amalgamated with 1% KBr and subjected to FTIR screening "Thermo Fisher, Nicolete IS10, Waltham, MA" in the 4000–450 cm^{-1} region.

2.6.2 Particle's sizes (Ps) and zeta (ζ) potential of nanomaterials. The Ps and ζ potential of the nanomaterials (Cht, NG/SeNPs, and Cht/NG/SeNPs) were appraised through DLS "Dynamic Light Scattering" approach, employing Malvern 3000 HS Zetasizer (Malvern, UK). Samples' solutions in DW (0.02%) were sonicated for 20 min at 23 Hz, and their Ps/ζ potentials were measured within −200 and +200 mV range at RT.

2.6.3 Electron microscopy screening. TEM (Transmission Electron Microscopy, Leica-Leo 0430; Cambridge, UK) and SEM (Scanning Electron Microscopy, JEOL, JSM-IT100, Tokyo, Japan) were employed for screening the Ps, morphology, and dispersion of NC (Cht/NG/SeNPs). For TEM appraisal, NC solution was sonicated for 12 min, dropped onto C-coated copper grids, vacuum-dehydrated for 28 min, and subjected to imagining at 20 kV. For SEM, the lyophilized NC of Cht, NG, and SeNPs were mounted onto a SEM self-adhesive disc, sputter-coated with gold and palladium, and examined at 8–10 kV.

2.6.4 Further characterizations of SeNPs. Additional characterization approaches, including the UV-visual spectroscopy analysis "Shimadzu, UV-2450, Japan" within 200–800 nm absorbance range; XRD analysis "X-ray diffraction, Shimadzu, XRD-6000, Japan" within 2θ of 10°–80° range; and SEM of plain SeNPs, were performed and their results are provided in the ESI.†

2.7. Antibacterial activity

2.7.1 Bacteria cultures. The antibacterial activity of NG, NG/SeNPs, Cht, and Cht/NG/SeNPs nanocomposite was evaluated, qualitatively and quantitatively, against standardized isolates of virulent food-borne bacteria. The cultures of *S. aureus*-ATCC25923, *S. Typhimurium*-ATCC14028, and *E. coli*-ATCC25922 were developed and challenged aerobically in NB (Nutrient broth) and NA (Nutrient agar) at 37 ± 1 °C. A standard antibiotic (Chloramphenicol) was employed for comparative antibacterial actions.[22]

2.7.2 Qualitative antibacterial assay: ZOI "inhibition zone". In order to rule out any possible effects of light on the activity of NPs, the qualitative examination (ZOI *via* disc diffusion) was applied in the dark. Spread bacterial cultures on NA plates were challenged with assay discs, which were placed on the surfaces of the inoculants. These discs contained 30 mL of (NG), (NG/SeNPs), Cht, and Cht/NG/SeNPs composite, each with a concentration of 100 μg mL^{-1}. The ZOI diameters were measured after 22 ± 2 h of incubation at 37 ± 1 °C; the ZOIs triplicated means were computed.[22]

2.7.3 Quantitative assessment: MIC "minimum inhibitory concentration". The MICs of NG, NG/SeNPs, Cht, and Cht/NG/SeNPs against challenged foodborne bacteria were evaluated *via* the micro-dilution method.[23] Bacterial cultures in NB (~4×10^7 CFU mL^{-1}) were confronted with successive concentrations of biocidal agents (within 10–100 μg mL^{-1} range) in microplates with 96 wells. The wells of incubated microplates (after 20 ± 2 h) were amended with *p*-iodonitrotetrazolium violet chromogenic indicator solution (4% w/v), which generates formazan red colour in alive cells. For confirming the biocidal action, 100 μL from wells that were suspected to have MICs (*e.g.*, colourless wells) were portions of wells spread onto plain NA plates for growth detection. The MICs were the lowest concentrations that could inhibit bacterial development in both microplates and NA plates.

2.7.4 Microscopic observation of treated bacterial strains. After being exposed to Cht/NG/SeNPs at their MIC values, *S.*

Typhimurium and *S. aureus* cells underwent morphological changes that might be used to determine the NPs action mode. Using a defined methodology, SEM imaging was performed.[24] The logarithmic-grown cells were treated with the NC for 4 and 8 h, collected with centrifugation (4700*g*), washed with neutral buffer, centrifuged again, dehydrated on SEM stubs, coated (gold or palladium), and then imaged to capture the apparent distortions and deformations in cells compared to the control.

2.7.5 ROS "reactive oxygen species" generation assay. For assessment of total ROS production from nanomaterials, grown bacteria (*S. aureus* and *S. Typhimurium*) cells were incubated with the 0.5 × MIC of plain SeNPs, NG/SeNPs and Cht/NG/SeNPs for 10 min, 30 min and 60 min. According to ROS Intracellular Assay Kit (OxiSelect™, STA-342; Cell Biolabs Inc., CA), samples were stained in dark for 30 min at RT and their fluorescence was measured using microplate reader at 525 nm emission and 488 nm excitation.

2.8. Antioxidant activity

FRAP "ferric reducing/antioxidant power" method was applied for judging the nanomaterials antioxidant activity. Portions of test samples (30 μL) were combined with DW (90 μL), then 900 L of FRAP reagent "comprised 25 mL of 0.3 M acetate buffer; pH 3.6; 2.5 mL of a 10 mM Ferrozine TM reagent in 40 mM HCl; and 2.5 mL of 20 mM $FeCl_3$–$6H_2O$" was freshly prepared and added. After holding the mixtures at 37 °C for 4 min, their absorbance was quantified at 595 nm using a microplate reader at RT.[25]

2.9. Treatment of fillets with nanocomposite edible coating

2.9.1 Poultry fillet preparation and treatment. Chicken fillets were freshly obtained from "Food Processing Research Plant, Kafrelsheikh University, Egypt", and transported to the laboratory at – 42 °C within 90 min. Poultry samples were divided into five categories, each with 510 cm slices of 2 cm thickness; the group had 20 slices. The untreated (DW-coated) group was the control group. The other groups used EC solutions containing 0.1% (w/v) of NG, NG/SeNPs, Cht, or Cht/NG/SeNPs. For coating experiments, poultry fillets were submerged in the coating solution for 1 minute and then permitted to drip the extra EC solution for 6 minutes before being re-immersed in EC solution for a further 30 seconds. Then left for aseptically draining on metal nets for 2 hours. EC-treated fillets were preserved at 41 °C for 14 days until the consequent quality estimations.[26]

2.9.2 Microbiological examination. The samples were prepared for bacterial detection by simply homogenizing 10 g of fillets' samples in 9 folds of sterile saline (0.85% NaCl). Following that, sequential numeric samples were diluted and loaded onto proper microbiological media. The whole microbiological assessments were done in triplicate, with the means recorded as log 10 CFU g^{-1}.[11,26]

To judge the effectiveness of EC treatment in protecting fillets from microbiological pathogens, various conventional procedures for microbiological analyses were used. According to standardized test methods, the following microbial groups and procedures were examined:

Escherichia coli, ISO 16649-1:2018.[27]

Staphylococcus aureus, ISO 6888-1:1999.[28]

Salmonella spp., ISO/TS 6579-2:2012.[29]

Psychrophilic bacterial count: ISO 17410:2019.[30]

2.9.3 Sensory evaluation. A trained panel of 10 individuals from the Department of Fish Processing and Biotechnology, Faculty of Fisheries and Aquaculture Sciences, Kafrelsheikh University, sensory evaluated treated raw chicken fillets and control samples. Participants were given samples to judge the food's general acceptability and quality, as well as its colour, flavour, smell, and texture. The samples were rated on a scale of 1 to 10. The samples with scores below 4 were rejected since it was believed by the shelf-life requirements that samples would be rejected if their sensory qualities were below a 4.

The examined sensory attributes and their grades were:

- Appearance: 1 = very decomposed; 10 = very healthy.
- Odour: 1 = very off-odours/unacceptable; 10 = very desired.
- Colour: 1 = very discoloured; 10 = no discoloration.
- Texture: 1 = very soft; 10 = compacted.
- Overall quality/acceptability: 1 = very unacceptable; 10 = very desirable.

2.10. Statistical analysis

Three assessments were made for each analysis in triplicated experiments, and standard deviations were calculated using Microsoft Excel 365. For statistical analysis of the significance of the data (at p 0.05), the SPSS (V-11.5, Chicago, IL) package's tests "*t*-test and ANOVA" were employed.

3. Results and discussion

3.1. Characterization of nanomaterials

3.1.1 Visual examination. The color of Na_2SeO_3 solution changed from pale yellow to orange-red when *P. oceanica* extract was 1%, followed by 1.5%, and finally 0.5%. The color intensity increased with time, but after 4 h, there were no more color alterations (Fig. 2).

The UV-vis spectrum of NG-mediated SeNPs (ESI; Fig. 1S†) appointed the appearance of one distinctive absorption peaks, *e.g.* at 272 nm, which indicates the homogeneity of phycosynthesized particles size and strongly associated with the distinctive SPR "Surface Plasmon Resonance" of biosynthesized SeNPs.[2,4,7,9,22]

Benhabiles *et al.*[20] also confirmed a change of colour from colourless to pale red in the biosynthesis of SeNPs using *Spirulina platensis* extract. The balls of *P. oceanica* are characterized by relatively high amounts of extractives and high cellulose content (40%), which resulted in the bioreduction of Na_2SeO_3 into red Se^0 and the biosynthesis of SeNPs.[1,7,9]

The XRD diffractogram of NG-mediated SeNPs (ESI; Fig. 2S†) appointed the detections of the distinctive peaks, *e.g.* the (002), (110), (202), (210), (211), (320), and (411), which signify the elevated crystallinity of the biosynthesized SeNPs.[2,4,7,9,22]

3.1.2 FTIR analysis. The infrared analysis of Cht (Fig. 3 Cht) revealed a band at 3426 cm^{-1} that was associated with strained intramolecular hydrogen bonds between O–H and N–H. Indicative of C–H symmetric and asymmetric stretching, the bands at 2921 cm^{-1} and 2872 cm^{-1}) are typical polysaccharide bands.[10,11]

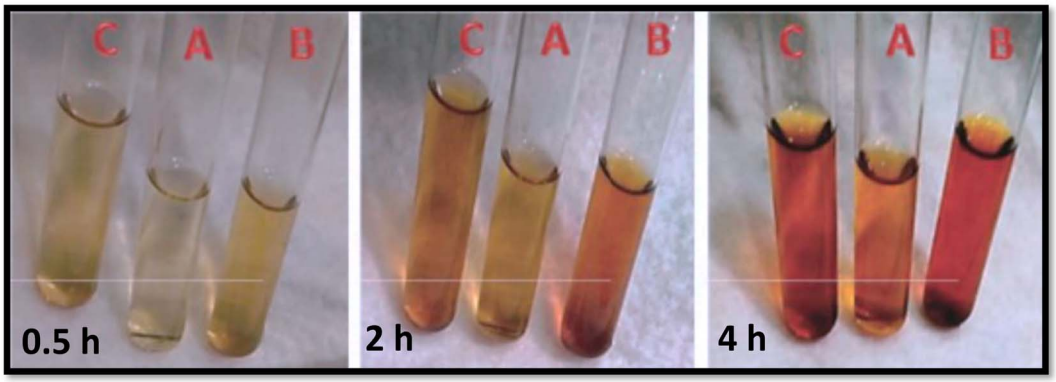

Fig. 2 The biosynthesis of SeNPs using 0.5% (A), 1.0% (B), and 1.5% (C) of *Posidonia oceanica* extract was confirmed by changes in the solution's colour from pale yellow to orange red after 0.5, 2, and 4 h.

Cht biological bonding can be distinguished by the following observed bands: 1153 cm^{-1} (bridge of asymmetric C–O–C stretching); 1067 cm^{-1} and 1024 cm^{-1} (stretched C–O); 1654 cm^{-1} (stretched C═O in amide I); 1321 cm^{-1} (vibrated stretching of C–N); 1412 cm^{-1} and 1357 cm^{-1} (CH_2 bending/CH_3 symmetrical deformations); the C–O overlapping and production of Cht after the interaction of NG and NH_4 groups in Cht molecules were revealed by the peaks that formed at 1153 cm^{-1} and 1066 cm^{-1}.[31]

Neptune grass extract (NG) infrared examination (Fig. 3: NG) revealed an expanded band within 3600–3000 cm^{-1}, indicating the presence of –OH and –NH vibrations. The steep peak at 1607 cm^{-1} specified the amide's –NH bond, while the peak at 1423 cm^{-1} appointed the deformation vibration of –C–OH with assistance from the carboxylate group's O–C–O symmetric stretched vibration, which is essential in the sorption of metal ions. The stretched O–O–C of the ester group is attributed to the peak at 1273 cm^{-1}. Alcoholic groups are responsible for the abrupt peak at 1046 cm^{-1}. As lignin, cellulose, and hemicelluloses are the main constituents of *Posidonia*, functional groups found in these substances can be the cause of several strong bands in FTIR spectra.[32,33]

The groups in NG (Fig. 3: NG/SeNPs) that are mainly responsible for the biosynthesis of SeNPs were identified by the combined NG/SeNPs spectral analysis. While the C–H band (at 2887 cm^{-1} in the NG spectrum) is mostly missed in the NG/SeNPs spectrum, signifying its roles in SeNPs conjugation and reduction, the band shift from 3426 cm^{-1} to 3482 cm^{-1} in the NG/SeNPs spectrum indicates Se interaction with N–H and O–H groups. From additional indications of the NG role in SeNP synthesis and reduction, the bands in the NG spectra at 1722 cm^{-1} (N–H of amides and carbocyclic groups) and at 1601 cm^{-1} (aromatic rings C═C) were markedly reformed. In the NG/SeNPs spectrum, the band at 1439 cm^{-1} (the aromatic rings in the NG spectrum) migrated to 1378 cm^{-1}. Additionally, the presence of several noticeable bands in the spectrum of NG/SeNPs at 1603 cm^{-1} and in the wavelength range of 756–812 cm^{-1} evidently verified the generation of novel vibrated bonds (mostly of Se–O) following interactions of Se with NG biomolecules.[34,35]

The involved functional groups in SeNPs interaction with Cht were detected with the aid of FTIR analysis, according to the infrared analysis of Cht/NG/SeNPs nanocomposites (Fig. 3: Cht/NG/SeNPs). A broad band at 3226 cm^{-1} was related to O–H stretching carboxylic acids. The formation of a very narrow band at 2878 cm^{-1} is attributed to C–H stretch alkanes. A tiny band at 1297 cm^{-1} showing the presence of aromatic amines with stretched C–N and nitro compounds with N–O symmetric stretching, and a small band at 1023 cm^{-1} caused by aliphatic amines with stretched stretch.[36]

The bio-organics from *P. oceanica* extract, including amino acids, esters, and unsaturated ketones' carbonyl and amide phytochemicals, were seen in FTIR to have been effective capping or reducing agents for SeNPs.[37]

3.1.3 Particle size and zeta potential (ζ) analysis. The synthesised nanomaterials' size and zeta potential are crucial physiochemical characteristics for NPs.[38] Table 1 exemplifies the mean Ps of NG/SeNPs, Cht, and Cht/NG/SeNPs at 12.41, 159.32, and 164.61 nm, respectively. Khoerunnisa *et al.*[39] stated that the particle size range of SeNPs was 3–18 nm. Ashraf *et al.*[40] reported that the mean diameter of chitosan NPs was 109.59 ± 10.11 nm, which was much greater than that of SeNPs. NCs have a larger particle size diameter than both SeNPs and nanochitosan because of fabricated NPs aggregation.[41]

ζ potential denotes the NPs surface charge that has a significant impact on the stability of selenium nanoparticles.[40–42] Table 1 presents the potential of SeNPs, Cht NPs, and Cht/NG/SeNPs nanocomposite were −34.2, +33.8, and +21.5 mV, respectively. Because of the positivity of amine groups' charging at low pH points, Cht can act as a cationic, water-soluble polyelectrolyte.[43] The reducing chemicals (phenolics acids and flavonoids) imparted SeNPs with a negative charged potential value present in bioorganic layer covering SeNPs biosynthesized by NG which have significant proportion of ionized carboxylic groups.[17–19] Negatively charged NPs are important in applications as antimicrobial agents.[44] Additionally, emulsions with absolute ζ potential variances >10 mV are suggested to have more stability, according to Kadu *et al.*[45] The favourable ζ potential range is (−30 to 20 mV or +20 to +30 mV).[46]

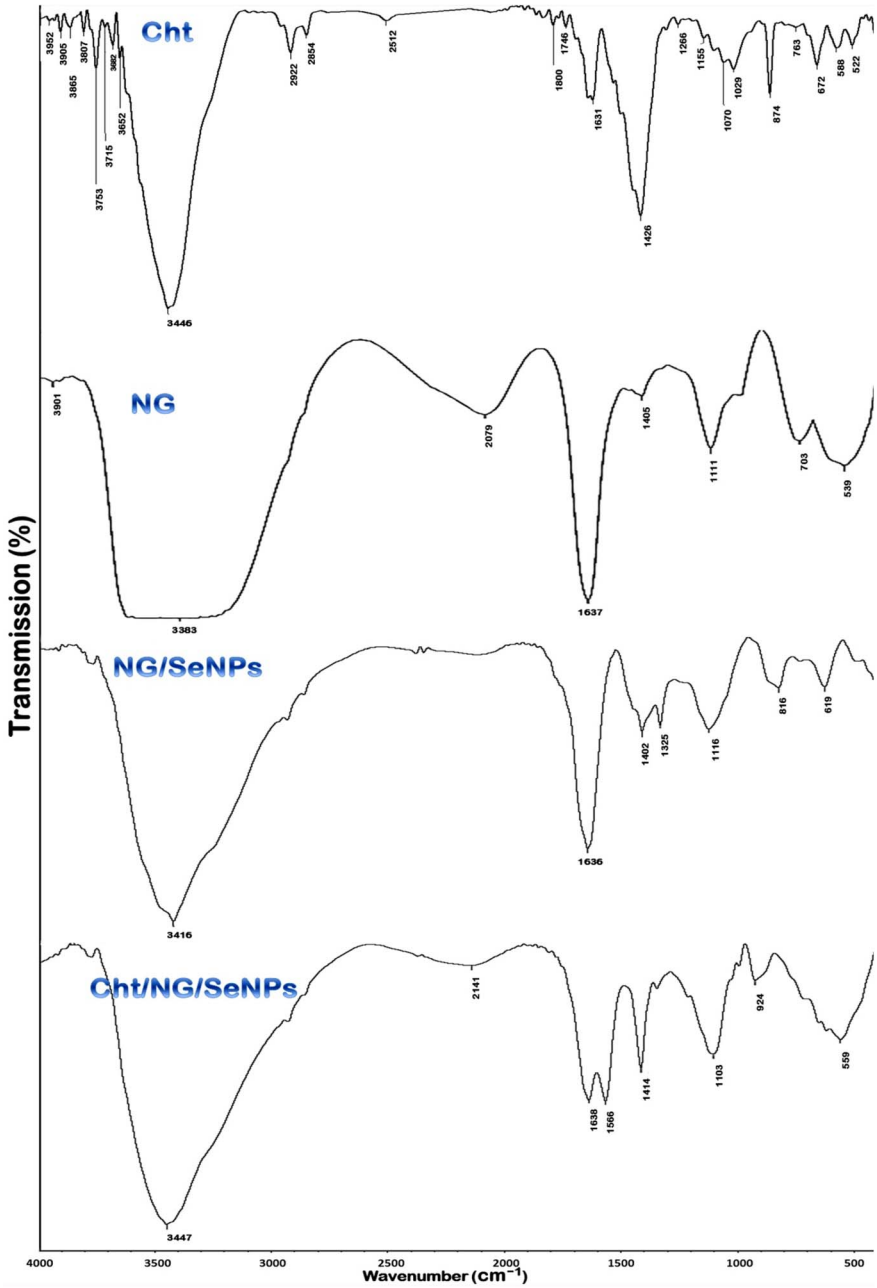

Fig. 3 FTIR analysis of nanochitosan (Cht), Neptune grass extract (NG), Neptune grass/SeNPs (NG/SeNPs), and Cht/NG/SeNPs nanocomposite.

Table 1 Size distribution and zeta charging of synthesized NG/SeNPs, chitosan NPs (Cht) and composite

Nanoparticles	Size range (nm)	Mean diameter[a] (nm)	ζ potential
NG/SeNPs	3.34–29.16	12.41[a]	−34.2 mV
Cht	73.15–274.22	159.32[b]	+33.8 mV
Cht/NG/SeNPs	85.11–260.38	164.61[c]	+21.5 mV

[a] Means of trials' triplicates; unalike letters (superscript) within a column designate significant difference ($p \leq 0.05$).

3.1.4 Electron microscopy analysis. The electron microscopy approaches were employed for visualizing the Ps, distributions, and shapes of NG and SeNPs (Fig. 4A) and their NC with Cht (Fig. 4B). TEM imagining demonstrated that synthesized NG and SeNPs were mostly spherical, with uniform Ps and distribution (Fig. 4A); their approximate Ps mean was 13.37 nm, which matches the attained results of DLS analysis. Harmonized findings were attained recently,[47] which reported the spherical shapes of biogenic SeNPs and a mean Ps 9.41 nm with minimal aggregation. The conjugation of Cht with NG/SeNPs could generate uniform NC particles with semi-spherical

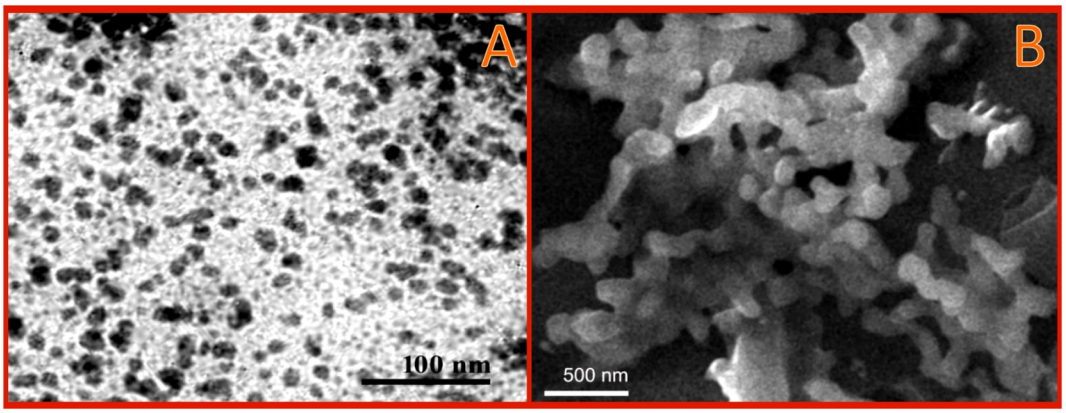

Fig. 4 Electron microscopy imaging of nanomaterials including TEM picture of SeNPs biosynthesized by *Posidonia oceanica* (A) and SEM of their conjugates with nanochitosan (B).

shapes and mean Ps diameters of 171.81 nm (Fig. 4B), which is slightly higher than attained values using DLS analysis. This is attributed to NC coating layers during SEM preparation.

The SEM analysis of plain synthesized SeNPs with NG- (ESI; Fig. 3S†) indicated the uniformity and homogenous distributions of phycosynthesized NPs; their average Ps was ~15.21 nm (*e.g.* slightly larger than the TEM results), which is generally attributed to the coating process of NPs with gold/palladium that results in NPs size increase.[4,7,9,46–48]

The Ps, shapes, and aggregation of biologically synthesized SeNPs are influenced by the nature of synthesizing biomolecules, which have different potentialities for reducing or capping SeNPs.[48] The phycosynthesized SeNPs using *Spirulina platensis* microalgae had Ps ranges from 2.8 to 38.9 nm,[22] whereas the biosynthesized SeNPs with *Catathelasma ventricosum* had Ps averages of 50 nm,[49] and those biosynthesized with raisin (*Vitis vinifera*) extract had a Ps range of ~3 to 18 nm.[50] This indicates the effectiveness of NG for reducing, stabilizing, and capping SeNPs.

3.2. Antimicrobial activity

3.2.1 *In vitro* antibacterial assessment. Using qualitative and quantitative assaying techniques, the *in vitro* antibacterial activity of Cht, NG, NG/SeNPs, and Cht/NG/SeNPs against *S. aureus*, *E. coli*, and *S. Typhimurium* is demonstrated in comparison to chloramphenicol (the standard bactericide) (Table 2). The entire panel of screened agents and NCs displayed impressive antibacterial activity against every bacterial isolate. The strongest agent was the nanocomposite (Cht/NG/SeNPs); it could outperform the other agents and standard chloramphenicol in terms of bactericidal activity. The antibacterial synergism of various agents was demonstrated because their combined effects (*e.g.*, NG/SeNPs and Cht/NG/SeNPs) were more effective than those of the individual drugs (*e.g.*, Cht and NG). *S. Typhimurium* was the most sensitive and *S. aureus* was the most resistant to challenging chemicals, as demonstrated *via* ZOIs and MICs values (Table 2) for every bacterial variety. All bacterial strains were remarkably susceptible to both NG/SeNPs and Cht/NG/SeNPs, while they were considered "moderately susceptible" towards plain Cht and NG.

The SeNPs deposit on the membrane of bacteria and negatively affects the cell division or bacterial survival.[50,51] Metal nanoparticles' antibacterial properties are related to the generation of ROS, hydroxyl radicals, hydrogen peroxide, and superoxide anions. These generated ROS can damage the bacterial cell membrane, prevent amine synthesis and DNA replication, and hinder the replication of proteins.[3,5,7,50] The diverse NG extracts were stated as potential bioactive agents with remarkable antimicrobial, anti-inflammatory, and antioxidant powers;[52,53] these broad activities of NG are correlated to

Table 2 Antibacterial activities of screened agents, Neptune grass extract (NG), (NG/SeNPs), nanochitosan (Cht), and their conjugates (Cht/NG/SeNPs), against food-borne pathogens, measured as ZOI "zone of inhibition, mm" and MIC "minimal inhibitory concentrations, μg mL^{-1}"

	Staphylococcus aureus		*Salmonella typhimurium*		*Escherichia coli*	
Antibacterial agent	ZOI[a]	MIC[b]	ZOI	MIC	ZOI	MIC
NG	8.7 ± 0.5^{a}	75.0	9.8 ± 0.7^{a}	70.0	9.7 ± 0.6^{a}	67.5
NG/SeNPs	14.8 ± 1.0^{c}	30.0	16.1 ± 1.4^{c}	25.0	15.6 ± 1.6^{c}	27.5
Cht	13.7 ± 1.2^{b}	35.0	15.7 ± 1.5^{b}	30.0	15.2 ± 1.4^{b}	32.0
Cht/NG/SeNPs	18.1 ± 1.3^{e}	25.0	19.8 ± 1.5^{e}	17.5	19.1 ± 1.2^{d}	20.0
Chloramphenicol	17.8 ± 1.4^{d}	25.0	19.9 ± 1.6^{d}	20.0	19.4 ± 1.5^{e}	17.5

[a] Values exemplify triplicated means ± SD "standard deviations"; "dissimilar superscript letters within the same column indicate significant difference at $p < 0.05$". [b] The used concentrations for MIC ranged from 10–100 μg mL^{-1}.

the presence of saponins, alkaloids, and tannins.[16,17,19,53,54] These actions are enhanced by transformation into nanoform, which increases the surface area and leads to more effective interaction and bactericidal activity.[55] The synergism in the Cht/NG/SeNPs composite leads to maximum bactericidal activity, as proved by the broadest ZOIs and tiniest MICs values; these forceful synergisms between Cht and other bioactive molecules from phytocompounds and nanomaterials were proved.[56–59]

3.2.2 Microscopic observation of treated bacterial cultures. The alteration in *S. Typhimurium* and *S. aureus* topography after exposure to MICs of Cht/NG/SeNPs was imaged using SEM (Fig. 5). In the beginning, the appeared bacterial cells have well preserved and intact cell walls (Fig. 5 – 0). After 4 h of exposure, the cells showed softening signs in their walls, with the appearance of notable distortions; the cells' interior constituents began to leak (Fig. 5 – 4). At the end of exposure, after 8 h, almost all treated *S. Typhimurium* and *S. aureus* cells were lysed; the few residual cell walls appeared in combination with leaked internal components and nanomaterials (Fig. 5 – 8).

3.2.3 The ROS generation. The nanomaterials (*e.g.* plain SeNPs, NG/SeNPs, and Cht/NG/SeNPs) were able to generate remarkable amounts of ROS within the treated bacteria (*S. aureus* and *S. Typhimurium*) during their incubation for 60 min. The ROS generations from nanomaterials were time-dependent and species-dependent (ESI; Fig. 4S†). The Cht/NG/SeNPs had the highest capability for ROS generation, followed by plain SeNPs, then NG/SeNPs. Additionally, the ROS production within *S. Typhimurium* was higher than the production within *S. aureus*. These findings match the former investigations,[3–5,7,50] which reported the elevated potentiality of SeNPs to generate ROS within biological cells.

3.3. Antioxidant activity

The antioxidant activity of NG, NG/SeNPs, and Cht/NG/SeNPs was evaluated compared to that of ascorbic acid (Table 3). All tested agents exhibited elevated antioxidant potentialities; the nanocomposite (Cht/NG/SeNPs) had the utmost activity, which significantly surpassed other agents and the standard ascorbic acid. The antioxidant synergism between conjugated agents was verified; the conjugation of various agents (NG/SeNPs and Cht/NG/SeNPs) exhibited more activity than the individual compounds (NG).

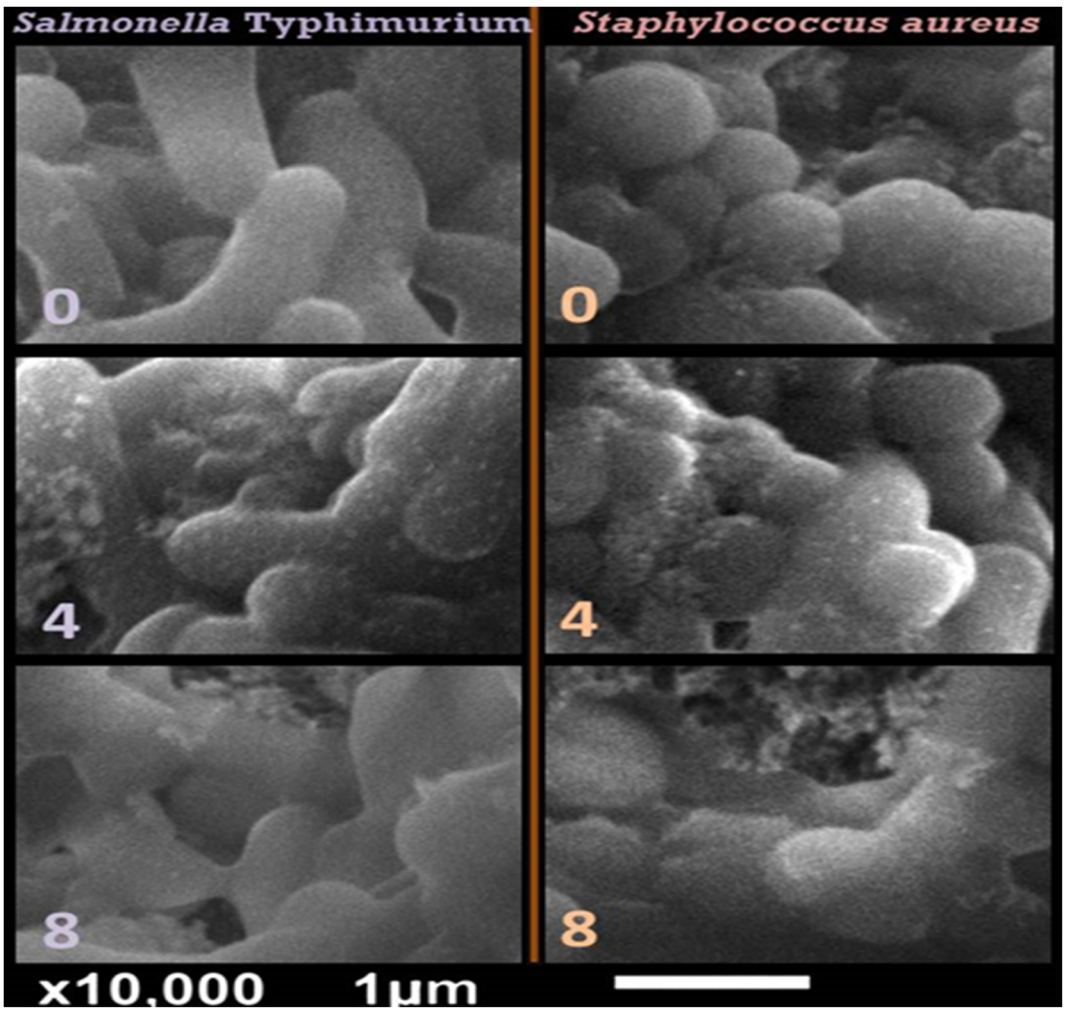

Fig. 5 SEM of treated *Salmonella* Typhimurium and *Staphylococcus aureus* with Cht/NG/SeNPs nanocomposite for (0, 4 and 8) h.

Table 3 Antioxidant activities of Neptune grass extract (NG), Neptune grass/SeNPs (NG/SeNPs), and their nanoconjugates with nanochitosan (Cht/NG/SeNPs)[a]

Compounds	Antioxidant activity (Rs%)
NG	47.51 ± 1.69^{a}
NG/SeNPs	79.45 ± 3.58^{b}
Cht/NG/SeNPs	91.36 ± 4.14^{d}
Ascorbic acid	89.14 ± 2.61^{c}

[a] Values exemplify triplicated means ± SD "standard deviations". "Dissimilar superscript letters within the same column indicate significant difference at $p < 0.05$".

The high phenolic and flavonoid content of Neptune grass is the reason of its antioxidant properties.[16,17,19,54] The scavenging of free radicals, inhibition of oxidase enzymes including NADPH oxidase and xanthine oxidase, and stimulation of antioxidant enzymes like superoxide dismutase and catalase are how phenolic chemicals work as antioxidants.[53,60]

3.4. Poultry fillets preservation with nanomaterials

3.4.1. Microbiological attributes. Table 4 demonstrates the impact of coating poultry fillets with the screened antimicrobial compounds or nanocomposites Cht group (B), NG group (C), NG/SeNPs group (D), and Cht/NG/SeNPs group (E) on the microbial counts of poultry samples.

The values of the microbial count of the control (acetic acid-dipped) group (A) were significantly high compared to other groups. The antimicrobial-coated fillet specimens could significantly maintain their microbiological attributes as compared to the control. When it came to preserving the characteristics of a fillet, the nanocomposites (NG/SeNPs and Cht/NG/SeNPs) considerably outperformed (NG and Cht).

The microbial count of psychrophilic bacterial count is crucial, especially in preserved foods kept at frigid temperatures.[61] It was recommended that the upper limit for psychrophilic bacteria be 4 log CFU g^{-1}. The items in the control group (A) were rejected after a short period of time, while the refusal in the group (C) happened on day 10, according to the results in terms of log CFU g^{-1} (Table 4). This indicates that the NG-treated group had a longer storage period due to the antimicrobial effect of NG extract phenolic acids. Due to the enhanced antibacterial effect of SeNPs, the E group continued to be appropriate up to the end of the investigation.[62–64]

The Cht/NG/SeNP coating reduced the quantity of psychrophilic bacteria to very low levels after storage, whereas the NG/SeNPs nanocomposite was also successful in reducing the microbial group count and halting the development of the different indicators of spoilage. These observations were formerly stated regarding Cht nanocomposites with phytocompounds and nanomaterials when they were applied as edible coatings for preserving diverse foodstuffs.[11,26,59,64,65]

3.4.2. Sensory evaluation. The effect of treatment with Cht group (B), NG group (C), NG/SeNPs group (D), and Cht/NG/SeNPs group (E) on sensory attributes of chicken fillet was illustrated in Table 5. Following the completion of an inferential statistical test, it was concluded that the greatest score for overall acceptability was recorded at day zero (9). The D and E groups stayed within the limit of acceptability until the end of the experiment, and the best results were in group E. Group A (control) was the most affected by microbial action and spoiled more quickly than other groups.

According to these findings, both group D (NG/SeNPs) and group E (Cht/NG/SeNPs) samples sustained outstanding sensory properties for a longer period of time with higher-grade sensory properties than the control group, but the panellists rejected the control samples in terms of odour, appearance, texture, colour, and overall acceptability (A). E group (Cht/NG/SeNPs) scores remained relatively stable throughout storage, which may indicate that the shelf life of poultry fillets could have been extended if the experiment had lasted longer than 14 days by applying this treatment.

3.4.3. Illustrations of coated poultry fillets with the tested composites throughout their 14 day cold storage at 4 °C. The impact of fillet treatments with nanocomposites' edible coating is emphasized in Fig. 6. For group A, bacteria that cause rotting can grow and cause flaws in items, including those with undesirable flavor, color, odor, texture, or appearance. On poultry surfaces kept at refrigerator temperatures, psychrotrophic spoilage bacteria proliferate, accumulating metabolic waste products or acting through extracellular enzymes (Fig. 6A).

As bacteria use the nutrients on the surface of meats, some of these metabolites can be detected by offensive odors. Rather than the protein breakdown in skin and muscle, small-molecule nitrogenous chemicals, such as amino acids, that exist in skin

Table 4 Microbial counts in treated fillets with antimicrobial compounds/nanocomposites, after preserving for 14 days at 4 ± 1 °C

	Microbial count[a] (log 10 CFU g^{-1})			
Coating material	*Staphylococcus aureus*	*Salmonella* spp.	*Escherichia coli*	*Psychrophilic* bacteria
Control (A)	8.77 ± 1.34^{d}	5.06 ± 1.03^{c}	3.94 ± 0.94^{c}	7.63 ± 1.34^{a}
Cht (B)	3.81 ± 0.37^{b}	1.65 ± 0.48^{b}	1.28 ± 0.44^{b}	6.20 ± 1.51^{a}
NG (C)	2.37 ± 0.43^{bc}	1.41 ± 0.53^{b}	1.12 ± 0.55^{b}	5.03 ± 0.45^{b}
NG/SeNPs (D)	1.79 ± 0.29^{c}	1.03 ± 0.46^{b}	ND[b]	4.08 ± 0.89^{c}
Cht/NG/SeNPs (E)	1.05 ± 0.19^{c}	ND	ND	3.61 ± 0.58^{c}

[a] Triplicates mans; similar superscript letters (in one column) indicate non-significance at $p < 0.05$. [b] ND: no apparent growth was detected.

Table 5 Sensory evaluation of antimicrobial-coated preserved poultry fillets after 14 days of cold storage at 4 °C (scores/10)

Sensory attributes	Storage period (days)	Coating material				
		Control (A)	Cht (B)	NG (C)	NG/SeNPs (D)	Cht/NG/SeNPs (E)
Appearance	0	9.3	9.6	9.0	8.5	8.9
	5	6.7	8.2	7.6	7.1	7.9
	10	4.2	6.8	6.2	6.4	7.1
	14	2.6	5.4	4.8	5.6	6.2
Odor	0	9.4	9.5	9.2	9.1	8.7
	5	5.9	7.9	7.1	7.4	7.9
	10	3.6	6.3	5.4	6.8	7.3
	14	1.1	5.5	4.3	5.3	6.6
Color	0	9.2	9.1	8.6	9.4	9.2
	5	6.7	7.6	6.4	8.3	8.6
	10	4.8	6.8	5.8	7.2	7.6
	14	3.2	6.1	5.2	6.5	7.1
Texture	0	9.4	9.6	9.1	9.2	8.8
	5	6.4	8.6	7.6	8.2	8.1
	10	4.7	7.3	5.7	7.1	7.6
	14	2.3	6.4	4.1	6.1	6.8
Overall quality	0	9.2	9.5	8.9	9.3	9.2
	5	5.8	8.1	7.7	8.0	8.6
	10	3.4	6.9	5.8	7.2	7.6
	14	1.3	6.3	4.6	6.6	7.1

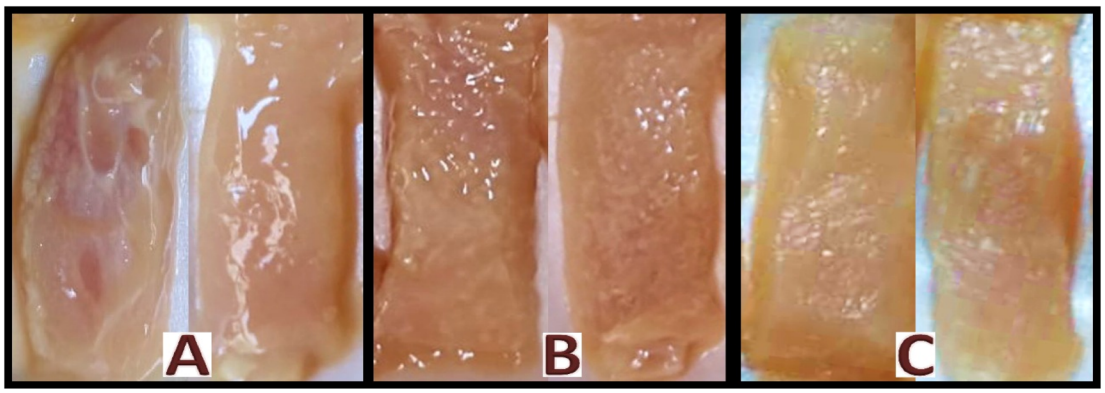

Fig. 6 Displays of coated chicken fillets, group A (acetic acid-dipped samples) (control), group B (NG/SeNPs), group C (Cht/NG/SeNPs), during cold storage for 14 days at 4 °C.

and muscle are directly used by microbes to produce off-odors. Along with the smell of dirty substances, poultry may start to decay in its final stages and develop an overwhelming ammoniacal smell. This smell may be caused by the breakdown of proteins and the creation of ammonia or ammonium-like chemicals.[63]

Regarding group B, poultry fillets coated with NG/SeNPs remained fresh for a longer period than in group A. The poultry tissues decompose and turn brown, and an unacceptable smell appears after 14 days, but it's not as unpleasant as in the control group (Fig. 6B).

For group C, poultry fillets coated with Cht/NG/SeNPs, the poultry fillet appears to have outstanding features compared to the other two sets. After 14 days of cold storage, the chicken fillets were in good condition, had a favourable smell, and had no visible symptoms of spoilage (Fig. 6C).

Low-temperature storage and the lack of a break in the cold chain can lengthen the shelf life of a product. If the temperature is dropped from 8.3 °C to 3.4 °C, the shelf life can even be doubled. Refrigeration can inhibit the growth of Enterobacteriaceae, which can generate acidic chemicals and deteriorate the organoleptic quality of poultry. Nevertheless, as the development of psychrotrophic bacteria is accelerated between 4 and 7 °C, using this combination will successfully shield food from deterioration or decay by microbial activity.[64,66,67]

4. Conclusion

This study demonstrated the successful biosynthesis of Cht, NG, and SeNPs with *P. oceanica* extract using a simple, economical, and environmentally outgoing nanobiotechnological approach,

as well as its use as an antibacterial and antioxidant agent. We can conclude that Cht/NG/SeNPs nanocomposites had potent antibacterial actions against Gram-positive/negative bacteria; the nanocomposite could burst, destroy, or deform bacterial cells, and their antibacterial impact was stronger in Gram-negative bacteria. It may be advised to use Cht, NG, or SeNPs as bio-preservatives in the food industry. To fully understand the workings of such types of Cht/NG/SeNPs nanocomposites' antibacterial and antioxidant capabilities, more research is necessary.

Author contributions

W. A. A. contributed in design of the work, investigation and analysis, work drafting; A. A. T. contributed in the conception, investigation, interpretation of data, supervision, work drafting; S. W. E. contributed in interpretation of data, resources, and fund acquistion; O. M. W. A. Data analysis. A. M. D. contributed in the conception, design of the work, investigation, analysis and supervision; O. M. A. contributed in the conception, interpretation of data, work drafting, revising and supervision; M. A. A. contributed in investigation and analysis, interpretation of data and work drafting; A. A. contributed in investigation and analysis, interpretation of data, writing, and submission. All authors contributed in editing, revising and approval of the submitted manuscript.

Data availability

All data generated or analysed during this study are included in this published article.

Conflicts of interest

The authors declare that they have no competing interests.

References

1 Y. Yu, P. Fan, J. Li and S. Wang, Preparation of Biocompatible Manganese Selenium-Based Nanoparticles with Antioxidant and Catalytic Functions, *Molecules*, 2023, **28**, 4498, DOI: **10.3390/molecules28114498**.

2 S. Rao, Y. Lin, R. Lin, J. Liu, H. Wang, W. Hu and T. Chen, Traditional Chinese medicine active ingredients-based selenium nanoparticles regulate antioxidant selenoproteins for spinal cord injury treatment, *J. Nanobiotechnol.*, 2022, **20**, 278, DOI: **10.1186/s12951-022-01490-x**.

3 A. Khurana, S. Tekula, M. A. Saifi, P. Venkatesh and C. Godugu, Therapeutic applications of selenium nanoparticles, *Biomed. Pharmacother.*, 2019, **111**, 802–812, DOI: **10.1016/j.biopha.2018.12.146**.

4 X. Xiao, H. Deng, X. Lin, A. S. M. Ali, A. Viscardi, Z. Guo, L. Qiao, Y. He and J. Han, Selenium nanoparticles: Properties, preparation methods, and therapeutic applications, *Chem.-Biol. Interact.*, 2023, **378**, 110483, DOI: **10.1016/j.cbi.2023.110483**.

5 V. Nayak, K. R. Singh, A. K. Singh and R. P. Singh, Potentialities of selenium nanoparticles in biomedical science, *New J. Chem.*, 2021, **45**(6), 2849–2878, DOI: **10.1039/D0NJ05884J**.

6 N. Zhang, Q. Ping, G. Huang, W. Xu, Y. Cheng and X. Han, Lectin-modified solid lipid nanoparticles as carriers for oral administration of insulin, *Int. J. Pharm.*, 2006, **327**(1–2), 153–159, DOI: **10.1016/j.ijpharm.2006.07.026**.

7 H. Hariharan, N. Al-Harbi, P. Karuppiah and S. Rajaram, Microbial synthesis of selenium nanocomposite using *Saccharomyces cerevisiae* and its antimicrobial activity against pathogens causing nosocomial infection, *Chalcogenide Lett.*, 2012, **9**(12), 509–515.

8 R. Y. Pelgrift and A. J. Friedman, Nanotechnology as a therapeutic tool to combat microbial resistance, *Adv. Drug Delivery Rev.*, 2013, **65**(13–14), 1803–1815, DOI: **10.1016/j.addr.2013.07.011**.

9 S. K. Torres, V. L. Campos, C. G. León, S. M. Rodríguez-Llamazares, S. M. Rojas, M. Gonzalez, C. Smith and M. A. Mondaca, Biosynthesis of selenium nanoparticles by *Pantoea agglomerans* and their antioxidant activity, *J. Nanopart. Res.*, 2012, **11**(3), 463, DOI: **10.3390/biology11030463**.

10 W. Chen, Y. Li, S. Yang, L. Yue, Q. Jiang and W. Xia, Synthesis and antioxidant properties of chitosan and carboxymethyl chitosan-stabilized selenium nanoparticles, *Carbohydr. Polym.*, 2015, **132**, 574–581, DOI: **10.1016/j.carbpol.2015.06.064**.

11 F. M. Almutairi, H. A. El Rabey, A. I. Alalawy, A. A. M. Salama, A. A. Tayel, G. M. Mohammed, M. M. Aljohani, A. A. Keshk, N. H. Abbas and M. M. Zayed, Application of Chitosan/Alginate Nanocomposite Incorporated with Phycosynthesized Iron Nanoparticles for Efficient Remediation of Chromium, *Polymers*, 2021, **13**, 2481, DOI: **10.3390/polym13152481**.

12 C. C. Ferreira Meneses, P. R. Monteiro de Sousa, K. C. N. Lima, L. M. M. de Almeida Souza, W. P. Feio and R. R. Claudio Marcio, Caffeic Acid-Zinc Basic Salt/Chitosan Nanohybrid Possesses Controlled Release Properties and Exhibits In Vivo Anti-Inflammatory Activities, *Molecules*, 2023, **28**, 4973, DOI: **10.3390/molecules28134973**.

13 R. Jha and R. A. Mayanovic, A Review of the Preparation, Characterization, and Applications of Chitosan Nanoparticles in Nanomedicine, *Nanomaterials*, 2023, **13**, 1302, DOI: **10.3390/nano13081302**.

14 H. Bahrulolum, S. Nooraei, N. Javanshir, H. Tarrahimofrad, V. S. Mirbagheri, A. J. Easton and G. Ahmadian, Green synthesis of metal nanoparticles using microorganisms and their application in the agrifood sector, *J. Nanobiotechnol.*, 2021, **19**, 86, DOI: **10.1186/s12951-021-00834-3**.

15 M. Vacchi, G. De Falco, S. Simeone, M. Montefalcone, C. Morri, M. Ferrari and C. N. Bianchi, Biogeomorphology of the Mediterranean *Posidonia oceanica* seagrass meadows, *Earth Surf. Processes Landforms*, 2017, **42**(1), 42–54, DOI: **10.1002/esp.3932**.

16 N. M. Ammar, H. A. Hassan, M. A. Mohammed, A. Serag, S. H. Abd El-Alim, H. Elmotasem, M. El Raey, A. N. El Gendy, M. Sobeh and A. H. Abdel-Hamid, Metabolomic

profiling to reveal the therapeutic potency of *Posidonia oceanica* nanoparticles in diabetic rats, *RSC Adv.*, 2021, **11**(14), 8398–8410, DOI: 10.1039/D0RA09606G.

17 M. Z. Haznedaroglu and U. Zeybek, HPLC Determination of Chicoric Acid in Leaves of *Posidonia oceanica*, *Pharm. Biol.*, 2007, **45**(10), 745–748, DOI: 10.1080/13880200701585717.

18 R. Khiari, Z. Marrakchi, M. N. Belgacem, M. F. Mhenni and E. Mauret, New lignocellulosic material: *Posidonia oceanica* for composite materials, *Compos. Sci. Technol.*, 2012, **71**, 1867–1872, DOI: 10.1016/j.compscitech.2011.08.022.

19 E. Barletta, M. Ramazzotti, F. Fratianni, D. Pessani and D. Degl'Innocenti, Hydrophilic extract from *Posidonia oceanica* inhibits activity and expression of gelatinases and prevents HT1080 human fibrosarcoma cell line invasion, *Cell Adhes. Migr.*, 2015, **9**(6), 422–431, DOI: 10.1080/19336918.2015.1008330.

20 M. S. Benhabiles, R. Salah, H. Lounici, N. Drouiche, M. F. Goosen and N. Mameri, Antibacterial activity of chitin, chitosan and its oligomers prepared from shrimp shell waste, *Food Hydrocolloids*, 2012, **29**(1), 48–56, DOI: 10.1016/j.foodhyd.2012.02.013.

21 H. Huang, Q. Yuan and X. Yang, Preparation and characterization of metal–chitosan nanocomposites, *Colloids Surf., B*, 2004, **39**(1–2), 31–37, DOI: 10.1016/j.colsurfb.2004.08.014.

22 B. E. ElSaied, A. M. Diab, A. A. Tayel, M. A. Alghuthaymi and S. H. Moussa, Potent antibacterial action of phycosynthesized selenium nanoparticles using Spirulina platensis extract, *Green Process. Synth.*, 2021, **10**(1), 49–60, DOI: 10.1515/gps-2021-0005.

23 A. A. Tayel, S. Moussa, K. Opwis, D. Knittel, E. Schollmeyer and A. Nickisch-Hartfiel, Inhibition of microbial pathogens by fungal chitosan, *Int. J. Biol. Macromol.*, 2010, **47**(1), 10–14, DOI: 10.1016/j.ijbiomac.2010.04.005.

24 T. J. Marrie and J. W. Costerton, Scanning and transmission electron microscopy of in situ bacterial colonization of intravenous and intraarterial catheters, *J. Clin. Microbiol.*, 1984, **19**(5), 687–693.

25 R. Pulido, L. Bravo and F. Saura-Calixto, Antioxidant activity of dietary polyphenols as determined by a modified ferric reducing/antioxidant power assay, *J. Agric. Food Chem.*, 2000, **48**(8), 3396–3402, DOI: 10.1021/jf9913458.

26 M. Haghighi and S. Yazdanpanah, Chitosan-based coatings incorporated with cinnamon and tea extracts to extend the fish fillets shelf life: Validation by FTIR spectroscopy technique, *J. Food Qual.*, 2020, **2020**, 8865234, DOI: 10.1155/2020/8865234.

27 British Standards Institution, *ISO 16649 -1: 2018, Microbiology of the Food Chain -Horizontal Method for the Enumeration of Beta-Glucuronidase-Positive Escherichia Coli*, BSI, London, UK, 2018.

28 British Standards Institution, *ISO 6888 -1:1999/Amd 2:2018, Microbiology of the Food Chain—Horizontal Method for the Enumeration of Coagulase-Positive Staphylococci (Staphylococcus aureus and other species)—Part 1: Technique Using Baird-Parker Agar Medium*, BSI, London, UK, 2018.

29 British Standards Institution, *ISO/TS 6579-2:2012, Microbiology of food and animal feed — Horizontal method for the detection, enumeration and serotyping of Salmonella — Part 2: Enumeration by a miniaturized most probable number technique*, BSI, London, UK, 2012.

30 British Standards Institution, *ISO 17410:2019, Microbiology of the food chain — Horizontal method for the enumeration of psychrotrophic microorganisms*, BSI, London, UK, 2019.

31 R. Varma and S. Vasudevan, Extraction, characterization, and antimicrobial activity of chitosan from horse mussel *Modiolus modiolus*, *ACS Omega*, 2020, **5**(32), 20224–20230, DOI: 10.1021/acsomega.0c01903.

32 E. Fortunati, F. Luzi, D. Puglia, R. Petrucci, J. M. Kenny and L. Torre, Processing of PLA nanocomposites with cellulose nanocrystals extracted from *Posidonia oceanica* waste: Innovative reuse of coastal plant, *Ind. Crops Prod.*, 2015, **67**, 439–447, DOI: 10.1016/j.indcrop.2015.01.075.

33 S. Boubakri, M. A. Djebbi, Z. Bouaziz, P. Namour, A. Ben Haj Amara, I. Ghorbel-Abid and R. Kalfat, Nanoscale zero-valent iron functionalized *Posidonia oceanica* marine biomass for heavy metal removal from water, *Environ. Sci. Pollut. Res.*, 2017, **24**(36), 27879–27896, DOI: 10.1007/s11356-017-0247-0.

34 C. Mellinas, A. Jiménez and M. D. Garrigós, Microwave-assisted green synthesis and antioxidant activity of selenium nanoparticles using *Theobroma cacao* L. bean shell extract, *Molecules*, 2019, **24**(22), 4048, DOI: 10.3390/molecules24224048.

35 S. Kannan, K. Mohanraj, K. Prabhu, S. Barathan and G. Sivakumar, Synthesis of selenium nanorods with assistance of biomolecule, *Bull. Mater. Sci.*, 2014, **37**(7), 1631–1635, DOI: 10.1007/s12034-014-0712-z.

36 J. Britto, P. Barani, M. Vanaja, E. Pushpalaksmi, J. Jenson Samraj and G. Annadurai, Adsorption of Dyes by Chitosan-Selenium Nanoparticles: Recent Developments and Adsorption Mechanisms, *Nat., Environ. Pollut. Technol.*, 2021, **20**(2), 467–479, DOI: 10.46488/NEPT.2021.v20i02.003.

37 H. J. Liu, C. H. Xu, W. M. Li, F. Wang, Q. Zhou, A. Li, Y. L. Zhao, Y. M. Ha and S. Q. Sun, Analysis of *Spirulina* powder by Fourier transform infrared spectroscopy and calculation of protein content, *Spectrosc. Spectral Anal.*, 2013, **33**(4), 977–981, DOI: 10.3964/j.issn.1000-0593(2013)04-0977-05.

38 I. Khan, K. Saeed and I. Khan, Nanoparticles: Properties, applications and toxicities, *Arabian J. Chem.*, 2019, **12**(7), 908–931, DOI: 10.1016/j.arabjc.2017.05.011.

39 F. Khoerunnisa, Y. D. Yolanda, M. Nurhayati, F. Zahra, M. Nasir, P. Opaprakasit, M. Y. Choo and E. P. Ng, Ultrasonic Synthesis of Nanochitosan and Its Size Effects on Turbidity Removal and Dealkalization in Wastewater Treatment, *Invent*, 2021, **6**(4), 98, DOI: 10.3390/inventions6040098.

40 M. A. Ashraf, W. Peng, Y. Zare and K. Y. Rhee, Effects of size and aggregation/agglomeration of nanoparticles on the interfacial/interphase properties and tensile strength of polymer nanocomposites, *Nanoscale Res. Lett.*, 2018, **13**, 214, DOI: 10.1186/s11671-018-2624-0.

41 M. Larsson, A. Hill and J. Duffy, Suspension stability; why particle size, zeta potential and rheology are important, *Annu. Trans.*, 2012, **20**, 209–214.
42 D. Natrajan, S. Srinivasan, K. Sundar and A. Ravindran, Formulation of essential oil-loaded chitosan–alginate nanocapsules, *J. Food Drug Anal.*, 2015, **23**(3), 560–568, DOI: 10.1016/j.jfda.2015.01.001.
43 F. Alexis, E. Pridgen, L. K. Molnar and O. C. Farokhzad, Factors affecting the clearance and biodistribution of polymeric nanoparticles, *Mol. Pharm.*, 2008, **5**(4), 505–515, DOI: 10.1021/mp800051m.
44 J. N. Losso, A. Khachatryan, M. Ogawa, J. S. Godber and F. Shih, Random centroid optimization of phosphatidylglycerol stabilized lutein-enriched oil-in-water emulsions at acidic pH, *Food Chem.*, 2005, **92**(4), 737–744, DOI: 10.1016/j.foodchem.2004.12.029.
45 P. J. Kadu, S. S. Kushare, D. D. Thacker and S. G. Gattani, Enhancement of oral bioavailability of atorvastatin calcium by self-emulsifying drug delivery systems (SEDDS), *Pharm. Dev. Technol.*, 2011, **16**(1), 65–74, DOI: 10.3109/10837450903499333.
46 Y. Liu, S. Zeng, Y. Liu, W. Wu, Y. Shen, L. Zhang, C. Li, H. Chen, A. Liu, L. Shen and B. Hu, Synthesis and antidiabetic activity of selenium nanoparticles in the presence of polysaccharides from Catathelasma ventricosum, *Int. J. Biol. Macromol.*, 2018, **114**, 632–639, DOI: 10.1016/j.ijbiomac.2018.03.161.
47 K. Kokila, N. Elavarasan and V. Sujatha, *Diospyros montana* leaf extract-mediated synthesis of selenium nanoparticles and their biological applications, *New J. Chem.*, 2017, **41**(15), 7481–7490, DOI: 10.1039/C7NJ01124E.
48 H. E. Touliabah, M. M. El-Sheekh and M. E. M. Makhlof, Evaluation of *Polycladia myrica* mediated selenium nanoparticles (PoSeNPS) cytotoxicity against PC-3 cells and antiviral activity against HAV HM175 (Hepatitis A), HSV-2 (Herpes simplex II), and Adenovirus strain 2, *Front. Mar. Sci.*, 2022, **9**, 1092343, DOI: 10.3389/fmars.2022.1092343.
49 P. A. Tran, N. O'Brien-Simpson, E. C. Reynolds, N. Pantarat, D. P. Biswas and A. J. O'Connor, Low cytotoxic trace element selenium nanoparticles and their differential antimicrobial properties against *S. aureus* and *E. coli*, *Nanotechnol*, 2015, **27**(4), 045101, DOI: 10.1088/0957-4484/27/4/045101.
50 H. A. Hemeg, Nanomaterials for alternative antibacterial therapy, *Int. J. Nanomed.*, 2017, **12**, 8211, DOI: 10.2147/IJN.S132163.
51 N. Filipović, D. Ušjak, M. T. Milenković, K. Zheng, L. Liverani, A. R. Boccaccini and M. M. Stevanović, Comparative study of the antimicrobial activity of selenium nanoparticles with different surface chemistry and structure, *Front. Bioeng. Biotechnol.*, 2021, **8**, 624621, DOI: 10.3389/fbioe.2020.624621.
52 N. Yuvaraj, P. Kanmani, R. Satishkumar, A. Paari, V. Pattukumar and V. Arul, Seagrass as a potential source of natural antioxidant and anti-inflammatory agents, *Pharm. Biol.*, 2012, **50**(4), 458–467, DOI: 10.3109/13880209.2011.611948.
53 M. A. Berfad, M. A. Fahej, A. Kumar and S. Edrah, Preliminary phytochemical and antifungal studies of sea grass, *Posidonia oceanica* obtained from mediterranean sea of Libya, *Int. J. Sci. Res.*, 2015, **4**, 30–33.
54 G. Castellano, J. Tena and F. Torrens, Classification of phenolic compounds by chemical structural indicators and its relation to antioxidant properties of *Posidonia Oceanica* (L.) Delile, *MATCH Commun. Math. Comput. Chem.*, 2012, **67**, 231–250.
55 Z. Ma, A. Garrido-Maestu and K. C. Jeong, Application, mode of action, and in vivo activity of chitosan and its micro-and nanoparticles as antimicrobial agents: A review, *Carbohydr. Polym.*, 2017, **176**, 257–265, DOI: 10.1016/j.carbpol.2017.08.082.
56 M. Soltanzadeh, S. H. Peighambardoust, B. Ghanbarzadeh, M. Mohammadi and J. M. Lorenzo, Chitosan nanoparticles as a promising nanomaterial for encapsulation of pomegranate (*Punica granatum* L.) peel extract as a natural source of antioxidants, *J. Nanomater.*, 2021, **11**(6), 1439, DOI: 10.3390/nano11061439.
57 M. Jiang, Y. Song, M. K. Kanwar, G. J. Ahammed, S. Shao and J. Zhou, Phytonanotechnology applications in modern agriculture, *J. Nanobiotechnol.*, 2021, **19**(1), 430, DOI: 10.1186/s12951-021-01176-w.
58 R. Javed, M. Zia, S. Naz, *et al.*, Role of capping agents in the application of nanoparticles in biomedicine and environmental remediation: recent trends and future prospects, *J. Nanobiotechnol.*, 2020, **18**, 172, DOI: 10.1186/s12951-020-00704-4.
59 M. F. Salem, W. A. Abd-Elraoof, A. A. Tayel, F. M. Alzuaibr and O. M. Abonama, Antifungal application of biosynthesized selenium nanoparticles with pomegranate peels and nanochitosan as edible coatings for citrus green mold protection, *J. Nanobiotechnol.*, 2022, **20**, 182, DOI: 10.1186/s12951-022-01393-x.
60 M. Mari, A. Colell, A. Morales, C. von Montfort, C. Garcia-Ruiz and J. C. Fernández-Checa, Redox control of liver function in health and disease, *Antioxid. Redox Signaling*, 2010, **12**(11), 1295–1331, DOI: 10.1089/ars.2009.2634.
61 R. Safari and M. Yosefian, Changes in TVN (Total Volatile Nitrogen) and psycrotrophic bacteria in Persian sturgeon Caviar (*Acipenser persicus*) during processing and cold storage, *J. Appl. Ichthyol.*, 2006, **22**, 416–418.
62 O. P. Fraser and S. Sumar, Compositional changes and spoilage in fish (part II)-microbiological induced deterioration, *Nutr. Food Sci.*, 1998, **98**(6), 325–329, DOI: 10.1108/00346659810235242.
63 S. Pons-Sánchez-Cascado, M. C. Vidal-Carou, M. L. Nunes and M. T. Veciana-Nogues, Sensory analysis to assess the freshness of Mediterranean anchovies (*Engraulis encrasicholus*) stored in ice, *Food Control*, 2006, **17**(7), 564–569, DOI: 10.1016/j.foodcont.2005.02.016.
64 M. M. Shehab, Z. I. Elbialy, A. A. Tayel, S. H. Moussa and Al-Hawary II, Quality Boost and Shelf-Life Prolongation of African Catfish Fillet Using Lepidium sativum Mucilage Extract and Selenium Nanoparticles, *J. Food Qual.*, 2022, **2022**, 9063801, DOI: 10.1155/2022/9063801.

65 A. A. Tayel, S. H. Moussa, M. F. Salem, K. E. Mazrou and W. F. El-Tras, Control of citrus molds using bioactive coatings incorporated with fungal chitosan/plant extracts composite, *J. Sci. Food Agric.*, 2016, **96**(4), 1306–1312.

66 S. Amjadi, S. Emaminia, M. Nazari, S. H. Davudian, L. Roufegarinejad and H. Hamishehkar, Application of reinforced ZnO nanoparticle-incorporated gelatin bionanocomposite film with chitosan nanofiber for packaging of chicken fillet and cheese as food models, *Food Bioprocess Technol.*, 2019, **12**, 1205–1219, DOI: **10.1007/s11947-019-02286-y**.

67 A. M. Youssef, H. S. El-Sayed, S. M. El-Sayed, M. Fouly and M. E. Abd El-Aziz, Novel bionanocomposites based on cinnamon nanoemulsion and TiO2-NPs for preserving fresh chicken breast fillets, *Food Bioprocess Technol.*, 2023, **16**(2), 356–367, DOI: **10.1007/s11947-022-02934-w**.